Midrapidity Hyperon Production in pp and pA Collisions

Carlos Merino

University of Santiago de Compostela
Galiza-Spain

(in collaboration with G.H. Arakelyan and Yu.M. Shabelski)

IS2014, Napa Valley, CA
3-7 December 2014

- Introduction

- Formalism of the Quark-Gluon String Model

- String Junction Contribution

- Inelastic Screening Effects

- Results and Discussion

See arXiv:1402.6505[hep-ph], and references therein.

- The Quark-Gluon String Model (QGSM) is based on Dual Topological Unitarization, Regge Phenomenology, and nonperturbative features of QCD.

- QGSM successfully describes multiparticle production in hadron-hadron and hadron-nucleus collisions.

- High energy interactions proceed via the exchange of one or several Pomerons, and elastic and inelastic processes result from cutting between or through Pomerons.

- The inclusive spectra of hadrons are related to the corresponding fragmentation functions of quarks and diquarks, constructed by using Reggeon counting rules.

- For the description of interactions with a nuclear target, the Gribov-Glauber Theory is used. The interaction is considered as the superposition of interactions with different numbers of target nucleons.

QGSM Formalism

Each exchanged Pomeron corresponds to a cylindrical diagram. When cutting one Pomeron, two showers of secondaries are produced
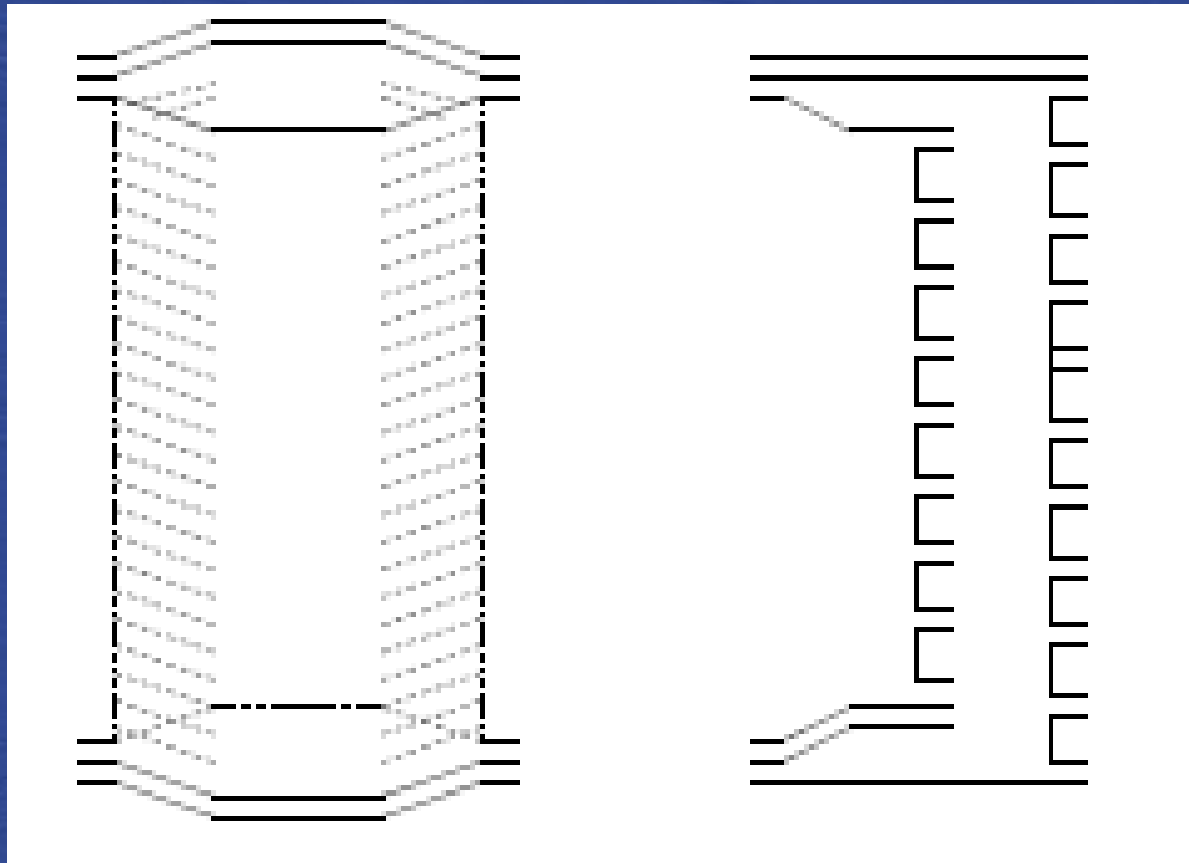
The inclusive spectrum of a secondary hadron h is then determined by the convolution of the diquark, valence quark, and sea quark distributions, u(x, n), in the incident particles, with the fragmentation functions, $G^h(z)$, of quarks and diquarks into the secondary hadron h.

Both the distributions and the fragmentation functions are constructed using the Reggeon counting rules.

In the case of multipomeron exchange, the distributions of valence quarks and diquarks are softened due to the appearance of a sea quark contribution.
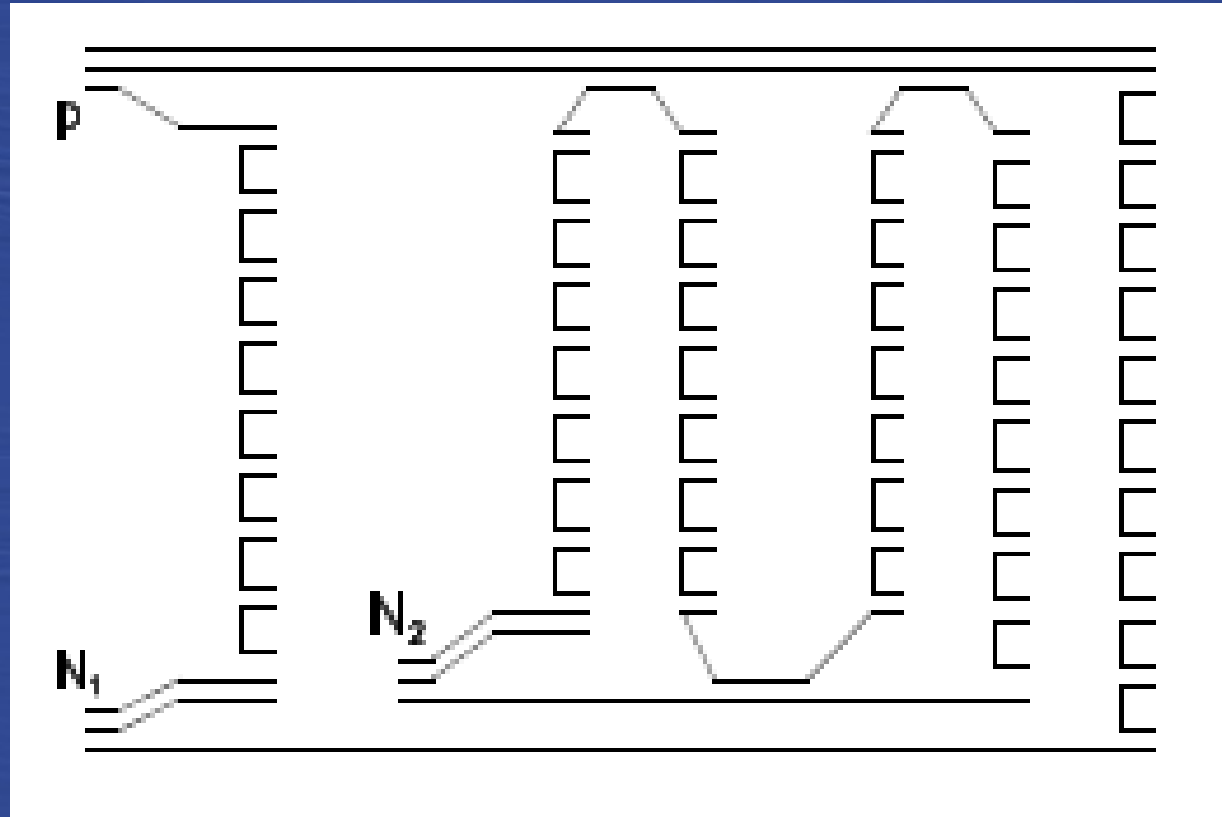
Every distribution $u_i(x, n)$ is normalized to unity.

For a nucleon target, the inclusive rapidity, y, or Feynman-x, x_F , spectrum of a secondary hadron h has the form

$$\frac{dn}{dy} = \frac{x_E}{\sigma_{inel}} \cdot \frac{d\sigma}{dx_F} = \sum_{n=1}^{\infty} w_n \cdot \phi_n^h(x)$$

where the functions $\varphi_n^h(x)$ determine the contribution of diagrams with n cut Pomerons, ω_n is the relative weight of these diagrams, and here we neglect the numerically small contribution of diffraction dissociation processes.

In the case of pp collisions:

$$\phi_n^h(x) = f_{qq}^h(x_+, n) \cdot f_q^h(x_-, n) + f_q^h(x_+, n) \cdot f_{qq}^h(x_-, n) + 2(n-1) \cdot f_s^h(x_+, n) \cdot f_s^h(x_-, n) \; ,$$

$$x_\pm = \frac{1}{2}[\sqrt{4m_T^2/s + x^2} \pm x] \; ,$$

where f_{qq}, f_q, f_s correspond to the contributions of diquarks, valence quarks, and sea quarks, respectively.

These contributions are determined by the convolution of the diquark and quark distributions with the fragmentation functions:

$$f_q^h(x_+, n) = \int_{x_+}^1 u_q(x_1, n) \cdot G_q^h(x_+/x_1) dx_1 \; .$$

In the calculation of the inclusive spectra of secondaries produced in pA collisions one has to consider the possibility of one or several Pomeron cuts in each of the ν blobs of the proton-nucleon inelastic interactions.

For example:

$$\frac{x_E}{\sigma_{prod}^{pA}} \cdot \frac{d\sigma}{dx_F} = 2 \cdot W_{pA}(2) \cdot w_1^{pN_1} \cdot w_2^{pN_2} \cdot \left\{ f_{qq}^h(x_+,3) \cdot f_q^h(x_-,1) + \right.$$

$$+ \quad f_q^h(x_+,3) \cdot f_{qq}^h(x_-,1) + f_s^h(x_+,3) \cdot [f_{qq}^h(x_-,2) + f_q^h(x_-,2) +$$

$$+ \quad 2 \cdot f_s^h(x_-,2)] \left. \right\} ,$$

is the contribution of the diagram in slide 6 to the inclusive spectrum, with $W_{pA}(2)$ the probability of interaction with two target nucleons.

All diagrams with every possible Pomeron configuration and its corresponding permutations have to be taken into account.

The total number of exchanged Pomerons becomes as large as

$$\langle n \rangle_{pA} \sim \langle \nu \rangle_{pA} \cdot \langle n \rangle_{pN} ,$$

where $\langle \nu \rangle_{pA}$ is the average number of inelastic collisions inside the nucleus (about 4 for heavy nuclei at SpS energies).

String Junction Contribution

In the string models baryons are considered as configurations (called String Junction) consisting of 3 connected strings related to the 3 valence quarks.

The production of a baryon-antibaryon pair in the central region usually occurs via SJ-$\overline{SJ}$ pair production, which then combines with sea quarks and antiquarks into a B$\overline{B}$ pair.
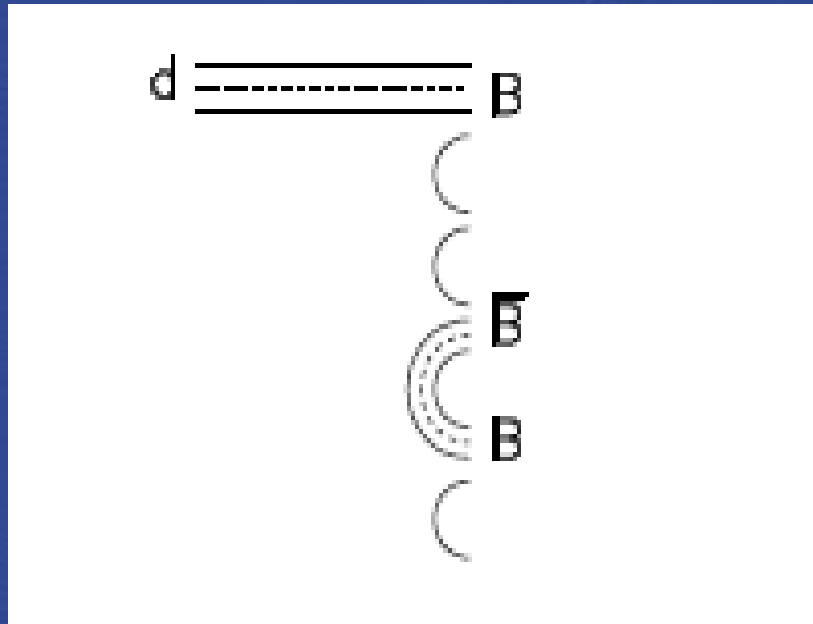
In the processes with incident baryons, another possibility to produce a secondary baryon in the central region (SJ diffusion in rapidity) exists
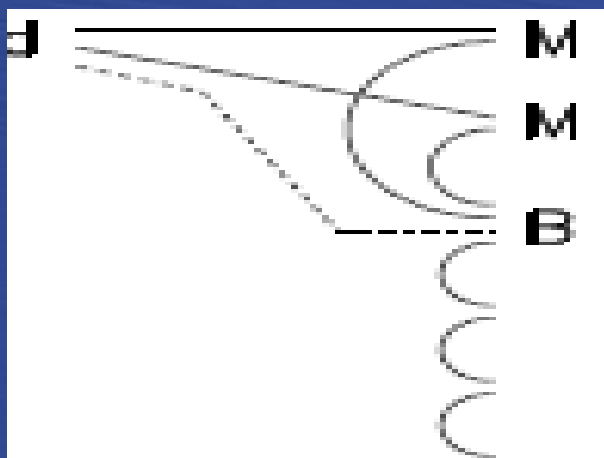
In QGSM, the differences at not very high energies in the spectra of secondary baryons and antibaryons appear for processes which present SJ diffusion in rapidity space.

These differences only vanish rather slowly when the energy increases.

The fragmentation functions for the secondary baryon B production can be written as follows:

$$G_{qq}^B(z) = a_N \cdot v_{qq}^B \cdot z^{2.5},$$

$$G_{qs}^B(z) = a_N \cdot v_{qs}^B \cdot z^2 \cdot (1-z),$$

$$G_{ss}^B(z) = a_N \cdot \varepsilon \cdot v_{ss}^B \cdot z^{1-\alpha_{SJ}} \cdot (1-z)^2,$$

where a_N is the normalization parameter, and $v_{qq}^B, v_{qs}^B, v_{ss}^B$ are the relative probabilities for different baryons production that can be found by simple quark combinatorics.

These probabilities depend on the strangeness suppression factor S/L, and we use S/L = 0.32.

The contribution of the SJ-diffusion graph has a coefficient, ε, which determines the small probability for such a baryon number transfer.

The fraction z of the incident baryon energy carried by the secondary baryon is smaller in the SJ-diffussion diagram.

Only these processes can contribute to the inclusive spectra in the central region at high energies if the intercept of the SJ exchange Regge-trajectory is large enough.

Our analysis gives a value of SJ = 0.5 ± 0.1, that is in agreement with the LHC result, SJ ~ 0.5, obtained by the ALICE Collaboration.

In the calculations of these effects we use the following values of the parameters

$$\alpha_{SJ} = 0.5 \text{ and } \varepsilon = 0.0757 .$$

Inelastic Screening Effects

The RHIC experimental data for Au+Au collisions give clear evidence of the inclusive density suppression effects which reduce by a factor ~0.5 the midrapidity inclusive density, when compared to the predictions based on the superposition picture.

This reduction can be explained by the inelastic screening corrections connected to multipomeron interactions.

At energies $\sqrt{s_{NN}} \leq 30{-}40$ GeV, the inelastic processes are determined by the production of one or several multiperipheral ladders, and the corresponding inclusive cross sections:
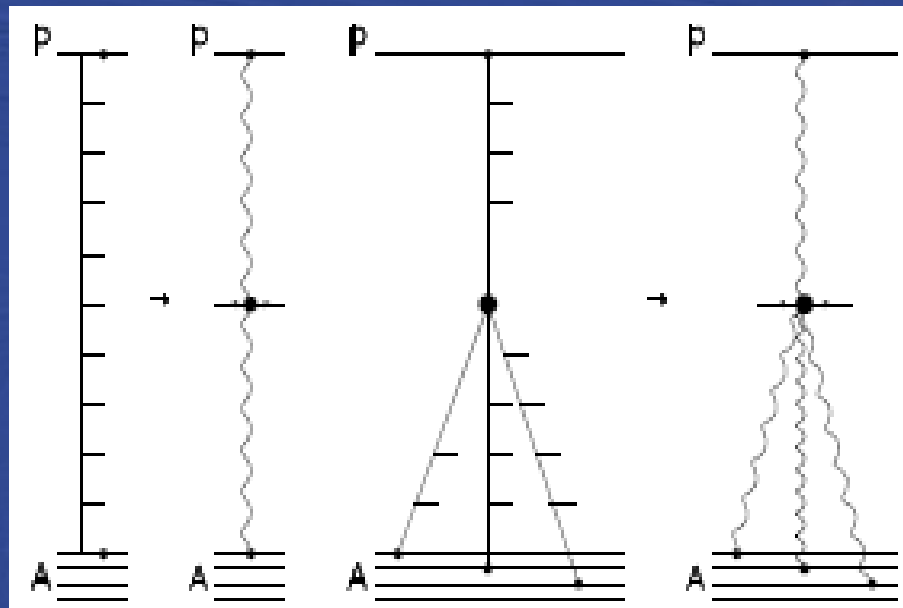
The fusion of multiperipheral ladders becomes more and more important with the increase of the energy, resulting in the reduction of the inclusive density of secondaries.

However, all quantitative estimations are model dependent.

 The numerical weight of the contribution of the multipomeron diagrams is rather unclear due to the many unknown vertices in these diagrams.

Percolation Effets

Another possibility to estimate the contribution of the diagrams with Pomeron interaction comes from Percolation Theory.

The percolation approach and its previous version, the String Fusion Model, predicted the multiplicity suppression seen at RHIC energies, long before any RHIC data were measured.

New calculations of inclusive densities and multiplicities in percolation theory both in pp, and in heavy ion collisions, are in good agreement with the experimental data in a wide energy region.

To account for the percolation effects in QGSM, it is more simple to consider the maximal number of Pomerons n_{max} emitted by one nucleon in the central region that can be cut.

These cut Pomerons then lead to the different final states.

The contributions of all diagrams with $n \leq n_{max}$ are accounted for as at lower energies.

The larger number of Pomerons $n > n_{max}$ can also be emitted obeying the unitarity constraint, but due to the fusion in the final state (at the quark-gluon string stage), the cut of $n > n_{max}$ Pomerons results in the same final state as the cut of n_{max} Pomerons.

Thus, all QGSM model calculations become very similar to the percolation approach.

The QGSM provides the integrated over p_T spectra of different secondaries as the functions of rapidity and x_F.

In this frame, we obtain a reasonable agreement with the experimental data on the inclusive spectra of secondaries produced in d+Au collisions at RHIC energy with a value n_{max} = 13, and in p+Pb collisions at LHC energy with the value n_{max} = 23.

It has been shown that the number of strings that can be used for the secondary production should increase with the initial energy.

Numerical Results

We compare the QGSM calculations with the experimental data, integrated over whole range of p_T, for energy the dependence until LHC energies, for Λ, $\bar{\Lambda}$, Ξ^-, Ξ^+ hyperons production density dn/dy ($| y | \leq 0.5$) in pp collisions.

$\sqrt{s}$ (GeV)	Reaction	QGSM	Experiment dn/dy ($|y| \leq 0.5$)
13.97 (102 GeV/c)	$p + p \rightarrow \Lambda$	0.024908	0.012 ± 0.01 [48]
14.075 (147 GeV/c)	$p + p \rightarrow \Lambda$	0.025095	0.0090 ± 0.0015 [49]
14.075 (147 GeV/c)	$p + p \rightarrow \bar{\Lambda}$	0.009833	0.057 ± 0.0044 [49]
19.42 (200 GeV/c)	$p + p \rightarrow \Lambda$	0.025582	0.0106 ± 0.006 [50]
19.42 (200 GeV/c)	$p + p \rightarrow \bar{\Lambda}$	0.011292	0.007 ± 0.0015 [50]
19.66 (205 GeV/c)	$p + p \rightarrow \Lambda$	0.025582	0.015 ± 0.0044 [51]
23.76 (300 GeV/c)	$p + p \rightarrow \Lambda$	0.026277	0.0076 ± 0.006 [52]
23.76 (300 GeV/c)	$p + p \rightarrow \bar{\Lambda}$	0.013051	0.015 ± 0.0076 [52]
27.6 (405 GeV/c)	$p + p \rightarrow \Lambda$	0.027049	0.0091 ± 0.0045 [53]
27.6 (405 GeV/c)	$p + p \rightarrow \bar{\Lambda}$	0.014530	0.017 ± 0.0041 [53]
200.	$p + p \rightarrow \Lambda$	0.045374	$0.0436 \pm 0.0008 \pm 0.004$ [54]
200.	$p + p \rightarrow \bar{\Lambda}$	0.039208	$0.0398 \pm 0.0008 \pm 0.0037$ [54]
200.	$p + p \rightarrow \Lambda(FD)$	0.045374	$0.0385 \pm 0.0007 \pm 0.0035$ [54]
200.	$p + p \rightarrow \bar{\Lambda}(FD)$	0.039208	$0.0351 \pm 0.0007 \pm 0.0032$ [54]
200.	$p + p \rightarrow \Xi^-$	0.005424	$0.0026 \pm 0.0002 \pm 0.0009$ [54]
200.	$p + p \rightarrow \bar{\Xi}^+$	0.004870	$0.0029 \pm 0.0003 \pm 0.006$ [54]
200.	$p + p \rightarrow \Omega^- + \Omega^+$	0.000903	$0.00034 \pm 0.00016 \pm 0.0005$ [54]
900.	$p + p \rightarrow \Lambda$	0.064856	0.26 ± 0.01 [55]
7000.	$p + p \rightarrow \Lambda$	0.098723	0.27 ± 0.01 [55]
900.	$p + p \rightarrow \Lambda$	0.064856	$0.108 \pm 0.001 \pm 0.012$ [56]
7000.	$p + p \rightarrow \Lambda$	0.098723	$0.189 \pm 0.001 \pm 0.022$ [56]
900.	$p + p \rightarrow \Xi^-$	0.008891	$0.011 \pm 0.001 \pm 0.001$ [56]
7000.	$P + P \rightarrow \Xi^-$	0.014968	$0.021 \pm 0.001 \pm 0.003$ [56]

Experimental data for strange baryons and antibaryons production in pp-collisions at different energies, from CERN SpS up to LHC, and the corresponding description by the QGSM.
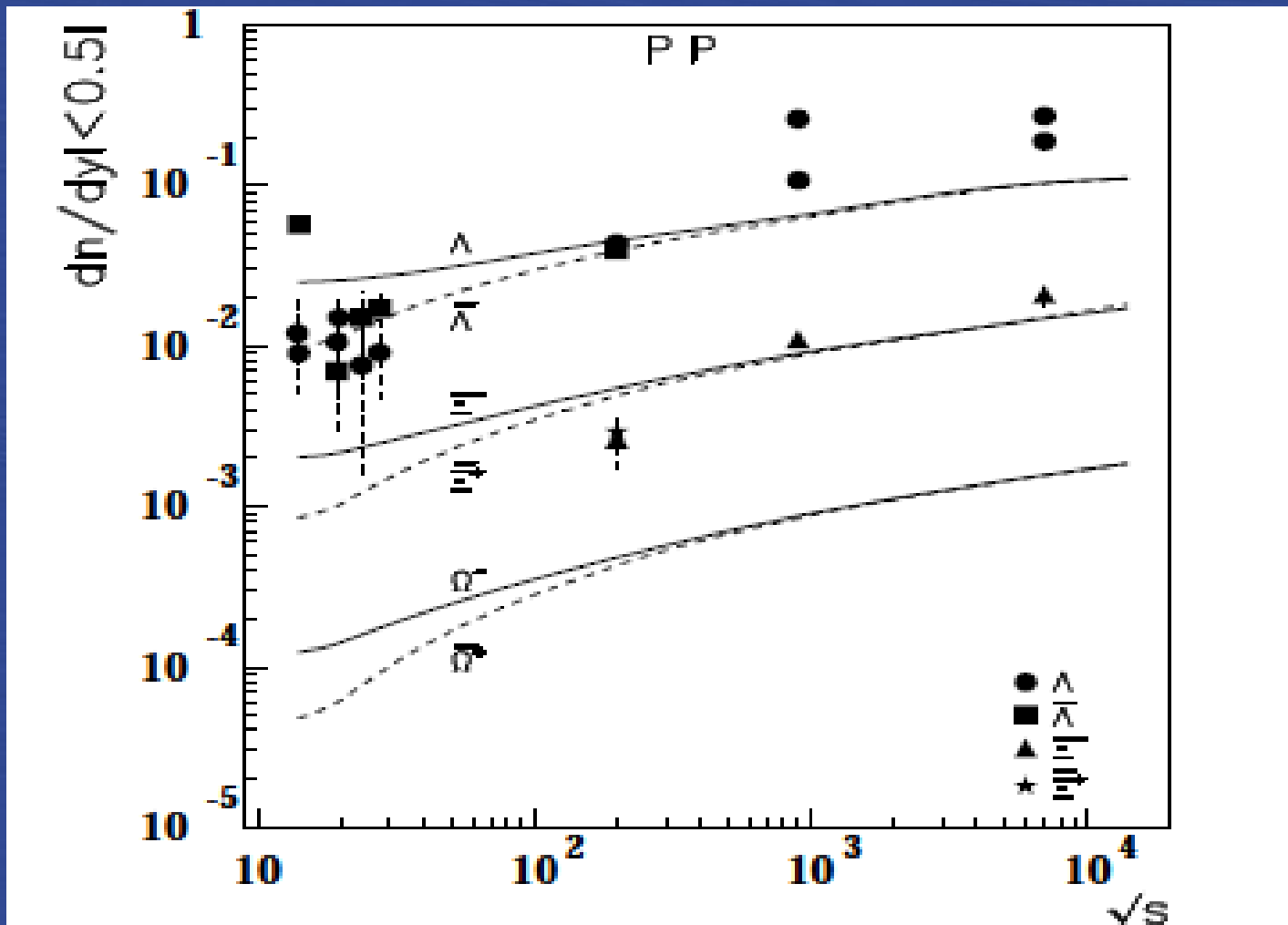
Energy dependence of hyperon production in midrapidity region, integrated over whole range of p_T, for pp collisions.
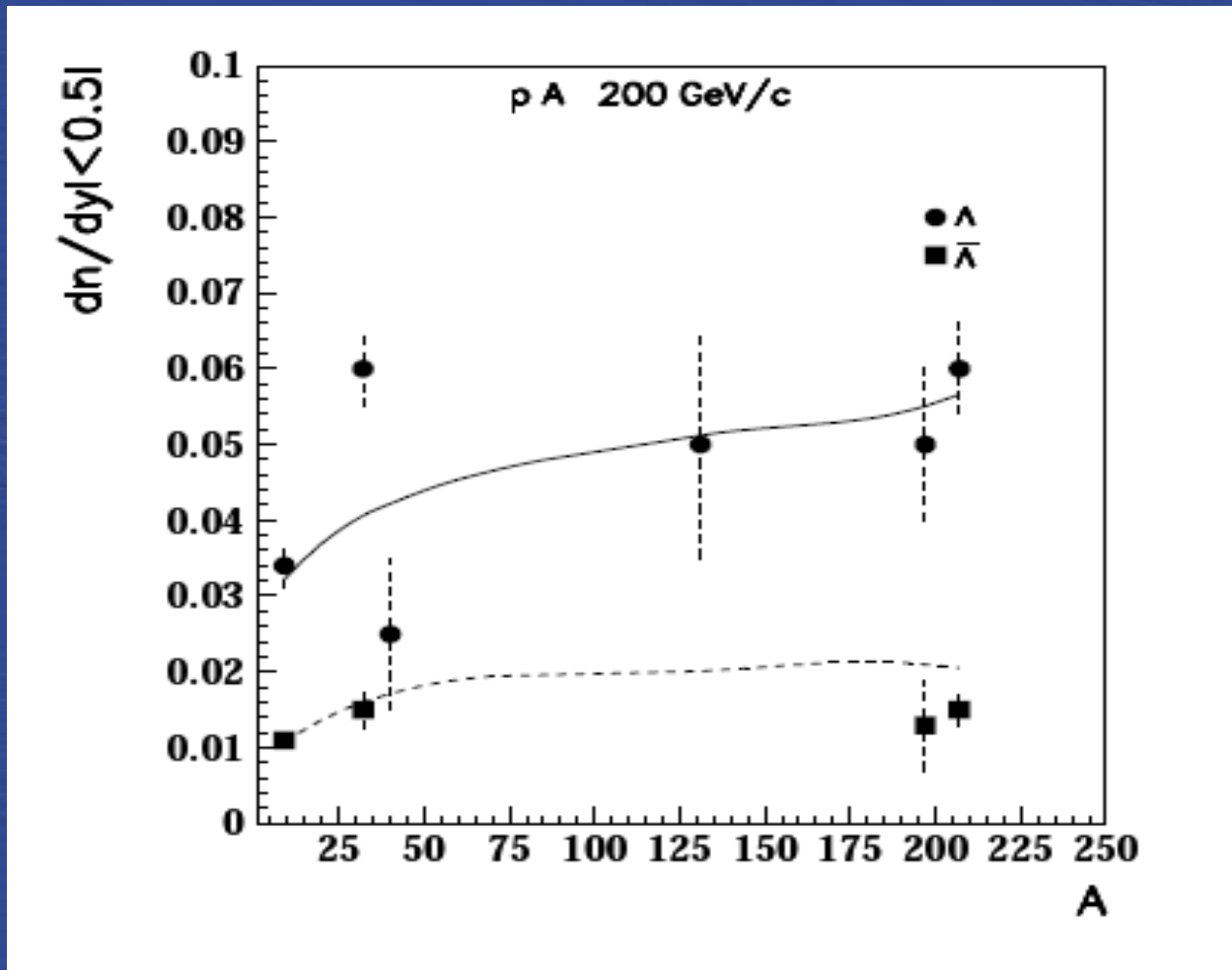
The full curves correspond to hyperon production and dashed curves to antihyperons production.

The absolute values of densities dn/dy($| y | \leq 0.5$) for Λ, $\bar{\Lambda}$

are higher than Ξ^-, and Ξ^+ densities about one order in large energy region up to LHC energies.

The same is also true for Ω^- and Ω^+ densities, in comparison with the Ξ^- and Ξ^+ densities.

| $\sqrt{s}$ (GeV)	Reaction	QGSM	Experiment $dn/dy(|y| \le 0.5)$
19.42 (200 GeV/c)	$p + Ar \to \Lambda$	0.0422	0.025 ± 0.01 [57]
19.42 (200 GeV/c)	$P + Xe \to \Lambda$	0.052	0.05 ± 0.015 [57]
19.42 (200 GeV/c)	$p + Au \to \Lambda$	0.055	0.05 ± 0.01 [58]
19.42 (200 GeV/c)	$p + Au \to \bar{\Lambda}$	0.021	0.013 ± 0.06 [58]
19.42 (200 GeV/c)	$p + S \to \Lambda$	0.0406	0.06 ± 0.005 [59]
19.42 (200 GeV/c)	$p + S \to \bar{\Lambda}$	0.016	0.015 ± 0.0025 [59]
17.2	$p + Be \to \Lambda$	0.0332	$0.034 \pm 0.0005 \pm 0.003$ [60]
(m.b.)	$p + Be \to \bar{\Lambda}$	0.0107	$0.011 \pm 0.0002 \pm 0.001$ [60]
17.2	$p + Pb \to \Lambda$	0.0554	$0.060 \pm 0.002 \pm 0.006$ [60]
(m.b.)	$p + Pb \to \bar{\Lambda}$	0.0188	$0.015 \pm 0.001 \pm 0.002$ [60]

Experimental data for strange baryons and antibaryons production in proton-nucleus collisions at different energies from CERN SpS up to LHC, and the corresponding description by the QGSM.

The A- dependences of the midrapidity density dn/dy of Λ and $\bar{\Lambda}$ hyperons produced at 200 GeV/c on nuclear targets.

The full curves correspond to hyperon production and dashed curves to antihyperons production.

The QGSM curves are in reasonable agreement with the experimental data.
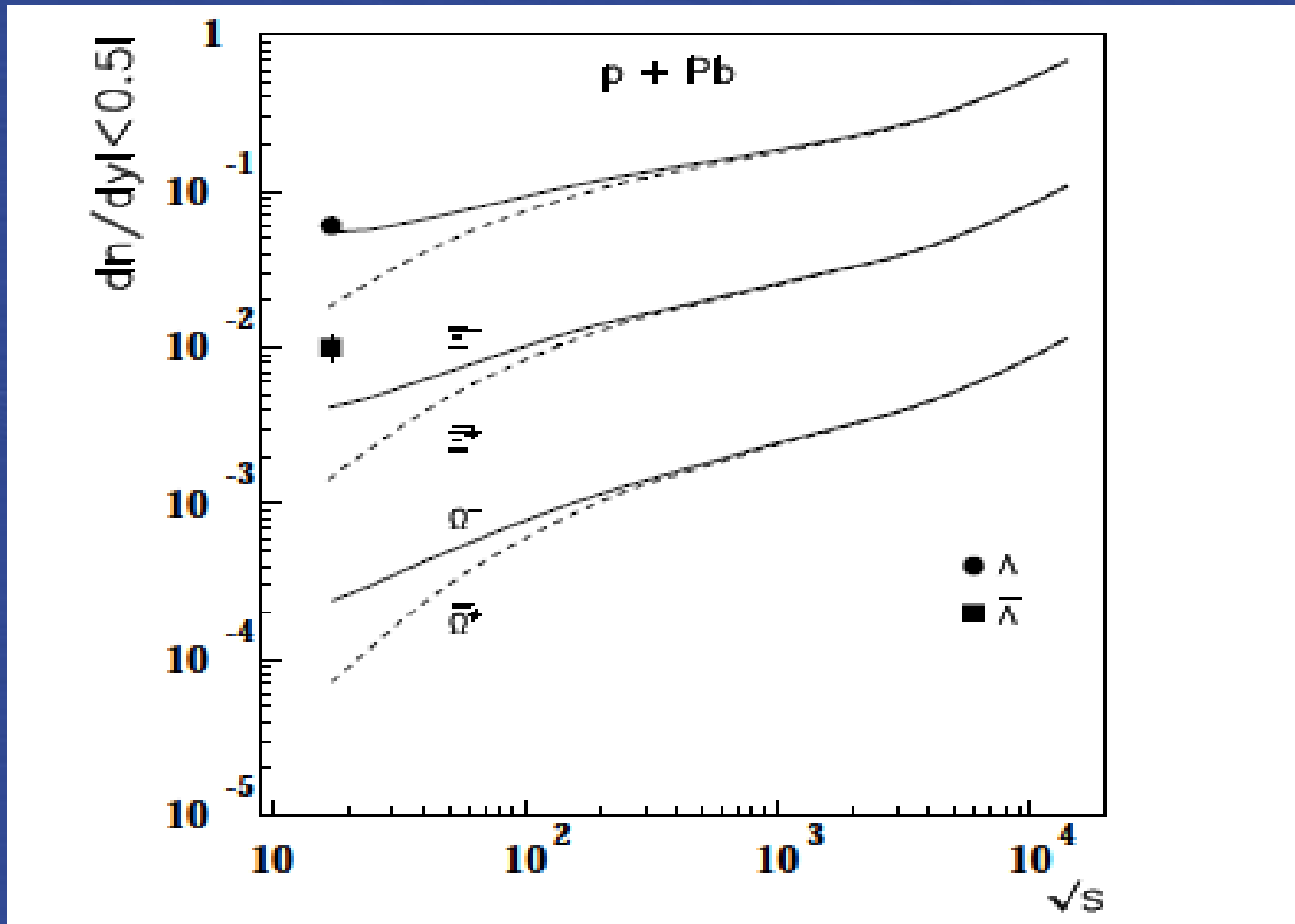
Energy dependence of hyperon production in midrapidity region for p-Pb collisions.

The full curves correspond to hyperon production and dashed curves to antihyperons production.

Conclusions

- The QGSM provides a reasonable description of strange and multistrange hyperons, as well as their antiparticles, production in pp and pA collisions at different energies.

- The QGSM predictions for the different hyperon productions in pp and p-Pb collisions are presented until LHC energies.

- A more detailed description (rapidity distributions, etc.) will be presented into the journal version.

- The description of the strange and multistrange baryon production in nucleus-nucleus collisions will be considered into a separate paper.